



The effect of extrusion and aging on the mechanical properties of additively manufactured AlSi10Mg

A. Ben-Artzy¹ · G. Hadad¹ · A. Bussiba² · M. Nahmany^{1,2}

Received: 11 October 2020 / Accepted: 26 September 2021 / Published online: 15 October 2021
© The Author(s), under exclusive licence to Springer Nature Switzerland AG 2021

Abstract

Additive manufacturing is used to build three-dimensional parts from a CAD model. The parts are layered constructed and selectively consolidated by laser or electron beam. This method enables the production of complex geometries of versatile materials parts. In this study, a powder laser bed fusion technique was used to create AlSi10Mg extrusion billets. The AM billets were subjected to stress relief heat treatment (HT) and hot extrusion process. The mechanical properties and microstructure of the extruded AM billets and aged hardened were evaluated. A significant improvement of the extruded sample's mechanical properties was found compared to cast and as-built material. In some cases, the yield stresses, tensile stresses, and elongation increased by 30–40%. Extrusion of additive manufactured billets can be used as a technique to gain better mechanical properties of heavy-duty products.

Keywords Extrusion · Mechanical properties · SLM · Additive manufacturing · AlSi10Mg

1 Introduction

1.1 Additive manufacturing

Additive manufacturing is used to create 3D parts by adding layers of materials and consolidating them by fusion in a computer-controlled system. This method allows the creation of various geometrical models using numerous materials such as polymers, metals, and ceramics. Additive manufacturing is based on planning using dedicated computer software, considering the (minimal) manufacturing constraints. High solidification rate and beam's hatching strategy defines the orientation, improves the microstructure and mechanical properties of the part. A typical scan speed of the melting laser beam (also present in the current study) is 0.5–1.5 m/s [1]. Nevertheless, the mechanical properties of AM parts are almost entirely anisotropic due to the building direction and suffer from porosity and rough surface. Many parameters involved in this technique all influence

the quality and properties of the final product. The energy of the heat source (i.e., electron-beam, laser, or friction), the hatching strategy (velocity and route of the beam), the beam diameter and energy density, and the environment are the parameters of the machine [2]. The chemical composition of the powder, particles' size, shape and distribution, are the powder parameters, along with the initial density of the dispensed powder [2–4]. The building strategy, route and the time between passes (cooling down of the workpiece) and substrate temperature are the parameters of the build, while heat treatment, surface treatment and HIP of the parts after the build are post-processing parameters.

1.2 Powder bed fusion by laser

Selective laser melting (SLM) is a technique where a laser beam is used to melt the metal powder layers during the building process. Similar to other AM techniques, this process is designed by dividing the model into very thin slices using software, to design the buildup strategy and route. The average particle size of the powder is typically 30–70 μm , while it is dispersed evenly over the metal substrate surface by a dispenser. A 200 μm in diameter and 350 W of energy laser beam selectively passes over the powder at a typical velocity of 900 mm/s and melts the areas of the build as required by design. Each pass of the beam melts few layers,

✉ A. Ben-Artzy
benartzyadi@gmail.com

¹ Materials Engineering Department, Ben-Gurion University,
P.O.B. 653, 8410501 Beer Sheva, Israel

² Materials Department, Nuclear Research Center,
P.O.B. 9001, 8419000 Beer Sheva, Israel

including the fresh new top powder layer. The whole process is carried out in the protective atmosphere of Argon to prevent oxidation of the powder and the melt and eliminate the dissolving of gases in the melted metal [2]. After the selective melting of the current layer is completed, the substrate stage is lowered by a thickness of less than one-layer thickness and the process repeat until the part is complete. The density of the SLM AM part can be very close to 100% [5], while the mechanical properties are usually equal or better than casted and aged conventional parts. The main advantages of the SLM method are that the parts are near-net-shape (NNS), display very fine grain size and have excellent mechanical properties. Parts can be manufactured from a variety of metals to build a complex geometry. The main disadvantages of SLM are a long time of manufacturing in comparison to other techniques, anisotropy structure and properties, some pores and rough surface.

1.3 Stress-relief heat treatment of AM parts

AM process is based on melting and rapid solidification of thin layers where each melts effect also the already solidified layers beneath it. This process is repeated, resulting in residual stresses (RS). Stress relieving heat treatments are commonly used in AM processes. Stress relieving heat treatment should consider internal gas pressure generated in pores and grain growth. Therefore, heat treatments are usually done at relatively low temperatures for short periods. A common stress relief heat treatment was performed successfully by [6] is 2 h @ 250 °C. In some cases, hot isostatic pressing (HIP) is used to decrease residual stresses and to reduce porosity (usually 0.8% after AM [5]). HIP is usually done at $0.8 \times T_M$ (beyond the recrystallization temperature) and in pressure higher than the material yield stresses. In some building strategies (material depending) stress relief is done by pre- or post-heating of the part using low energy beam. In some cases, the annealing of residual stresses is done using a second laser beam. Pre-heating the substrate, heating the metal powder or the vicinity of the melted pool by a second laser is done to decrease the temperature gradient [7]. It has been shown that using a multi-beam strategy in SLM was efficient in RS reduction [8]. Building parts

on a hot substrate is also a common technique to decrease residual stresses in the final AM product.

1.4 AlSi10Mg alloy

AlSi10Mg alloy is commonly used to cast complex parts with higher wall thickness, designed for heavy loads in automotive and aviation, chemicals and food industries. This alloy can be cast in various techniques, such as high-pressure die-casting or sand mold casting. Castings used in aluminum alloys are usually characterized by defects, overcome by Silicon addition and more alloying elements, which improves the mechanical properties of the cast. The binary high magnesium alloys Al-Si are age-hardening alloys and thus improved mechanical properties by heat treatment. The aging process is based on β (Mg_2Si) precipitates, thus contributes to strength. The precipitation creation is based on the limited solubility of aluminum and Silicon and the eutectic point of 12.6 wt% Si at 577 °C. Therefore, AlSi10Mg is a commonly used alloy for AM technique. According to [5], the typical density of AM AlSi10Mg alloy is 2.66 gr/cm³, while the theoretical density is 2.68 gr/cm³. Typical mechanical properties of AlSi10Mg alloy are listed in Table 1. The comparison between different manufacturing techniques to AM (in XY and Z building direction) emphasize the advantage of AM over other techniques [6, 9–11]. One should note that other techniques listed in Table 1 are in the aged (T6) condition while AM is presented in the as-built condition. Typical mechanical properties [9] of AM-AlSi10Mg specimens with relatively similar chemical compositions are presented in Table 2.

1.5 Extrusion

Extrusion is a well-known process that can be done using different techniques (direct, indirect or backward). A hydraulic press is used to produce long solid or hollow profiles, characterized by a constant cross-section. The product of the extrusion process is a near net shape (NNS) product. The extrusion of metals is usually done at a temperature above the recrystallization temperature ($\sim 0.6 T_m$), where deformation is mostly carried out by grain boundary sliding (GBS). At this temperature, the flow stress of the metal is

Table 1 Typical mechanical properties of AlSi10Mg [6, 10, 11]

Process	Manufacturing process/direction	<i>E</i> , GPa	TS, MPa	ϵ_f , %	HV
Additive manufacturing	XY direction	68	391	5.55	127
	Z direction	N/A	396	3.47	N/A
Casting	Conventional cast and aged T6	71	300–317	2.5–3.5	86
	High pressure die-casting As-cast	71	300–350	3–5	95–105
	High pressure die-casting and aged T6	71	330–365	3–5	130–133

Table 2 Typical mechanical properties of AlSi10Mg (Al 10wt% Si 0.45 wt%Mg) AM Vs. casting specimens with relatively similar chemical compositions [9]

Process	YS [MPa]	TS [MPa]	Elongation [%]	Thermal condition	Build direction*
Additive manufacturing	184	288	7.2	2 h at 300 °C	Z direction
	182	282	7.6	2 h at 300 °C	XY direction
	180	287	14.3	2 h at 300 °C	Z direction
	182	285	17.9	2 h at 300 °C	XY direction
	220	325	7	2 h at 300 °C	Z direction
	220	335	11	2 h at 300 °C	XY direction
EN AC casting	80	150	2	As-cast	Alternative name 43000
	180	220	1	Cast and aged T6	Alternative name 43000

low, and the strain hardening coefficient is negligible, which enhances formability. Extrusion at moderated temperature decreases pores size, improves surface quality and improves mechanical properties due to the massive plastic deformation. The metal flow is parallel to the extrusion direction in “direct extrusion” process, while in “indirect extrusion” it flows backward thru a hollow stem die [2, 3].

Originally, AM processes were used to manufacture prototypes, currently being used in both prototyping and end-use complex and unique products manufacturing. It is not common to use AM to produce billet for secondary fabrication processes like extrusion. Since grain size of final product influences the mechanical properties according to Hall–Petch law, much efforts are invested by researchers to decrease grain size using ECAE, reciprocal extrusion and other techniques. The idea behind this research was to take advantage of the orderly fine grain size of AM metals to increase the strength of the final product made by extrusion process. It was impossible to estimate theoretically the influence of the AM building orientation on the mechanical properties of the extruded parts.

1.6 Previous work

In previous similar research hot workability of SLM Ti-6Al-4 V and Ti–Al alloys was evaluated by elevated temperature compression tests [12, 13]. Ti-6Al-4 V Components were build using WAAM and hot rolled in [14]. Ring rolling raw material was made using WAAM to increase the flexibility of the process [15]. Previous papers are reporting that microstructure was refined during hot working due to recrystallization. No signs of damage were found in the compressed samples, and the character of the strain hardening behavior shows modifications from the as-cast alloys. It

was reported that much lower flow stress values were found in comparison to conventional cast + HIPed material, while flow stress was reduced by more than 40%. WAAM pre-forms showed good forming behavior and the combination of WAAM and ring rolling seems viable to improve process efficiency. One of the important findings was a significant influence on mechanical properties regarding orientation and process route. The authors did not find any previous work regarding the hot extrusion of SLM AM alloys.

2 Experimental

2.1 Additive manufacturing of the samples

AM-AlSi10Mg extrusion billets were built by SLM EOSINT M280 machine, using 70 µm pre-alloyed powder with chemical composition as shown in Table 3, according to standard DIN EN 1706:2010. Extrusion billets of 30 mm long and 14 mm in diameter were built in X–Y, Z and 45° orientation (A). The general built orientations are illustrated in Fig. 1a. The substrate has beam rotated 67° between layers passes to reduce the anisotropic nature of the process in the X–Y plane. The red arrow in Fig. 1a designates the building direction Z. The as-build extrusion billets can be seen in Fig. 1b, marked with their building directions. All AM billets were stress-relieved and machined to 12 mm in diameter to remove any roughness, oxides or defects on the billet surface before extrusion.

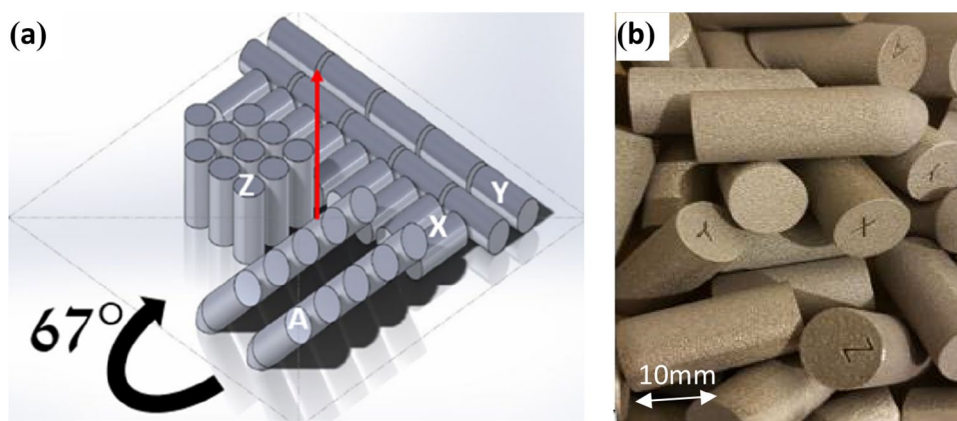
2.2 Extrusion of AM billets

Extrusion of the AM billets was done using a micro indirect hydraulic extrusion press located in the Ben-Gurion

Table 3 Chemical composition of AM AlSi10Mg extrusion billets

Element	Si	Mg	Fe	Mn	Cu	Zn	Ti	Al
(wt%)	10.2	0.4	0.1	0.001	0.003	0.002	0.002	Balance

Fig. 1 Building scheme and extrusion billets; **a** building strategy and X, Y, Z, A orientations **b** AM billets in very orientations



university laboratory (Fig. 2a). This apparatus allows a controlled temperature—forces extrusions of light metals using different types of dies (Fig. 2b). Indirect extrusion was selected for this work since the lack of friction between the billet and the container. This friction might increase the extrusion force and influence the metal flow in the common (forward) extrusion technique. Nevertheless, the replacement of dies (stem) in indirect extrusion is much easier. To minimize grain growth, the AM billets' extrusions were performed after a short soaking time at 300 °C. The friction was reduced using Mo₂S lubricant. The extrusion speed was 13 mm/s, while the extrusion ratio was 5.4, resulting in 6 mm in diameter bars. Extruded bars, made out of different build directions billets, are seen in Fig. 2c.

2.3 Heat treatments

The SLM as AM samples were stress-relieved at 300 °C for 2 h. The purpose of this heat treatment was to relieve any residual stresses that might have been presented in the extrusion billets as a consequence of the AM process.

The AM extruded bars' age-hardening heat treatment was performed by solution heat treatment (SHT) 510 °C for 6 h, followed by aging at 170 °C for 4 h [2] as AM material was also aged for comparison reasons.

2.4 Characterization

The extruded samples were cut perpendicularly to the extrusion direction, polished (down to 1 μm), and etched in 48% HBF₄ solution. The samples were examined by optical microscopy (OM), scanning electron microscopy (SEM) and EDS for chemical composition analysis. VH micro-hardness (2000 N load) tests were performed on the as extruded samples. The mechanical properties were evaluated using 4 mm gauge diameter over 16 mm in length tensile tests samples according to ASTM: E8/E8M standard at a strain rate of 0.01/s. using Instron 5982 frame apparatus equipped with “Blue hill” software for control and analysis. SEM fractography investigation was conducted on broken tensile test samples.

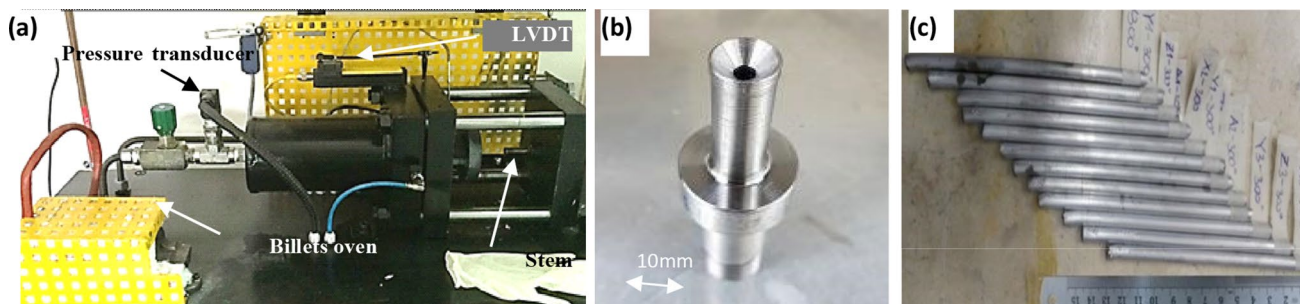


Fig. 2 Extrusion press set-up; **a** laboratory hydraulic extrusion press, **b** 6 mm conical 120° die **c** extruded 6 mm bars obtained from different billets orientations

3 Results and discussion

3.1 Microstructure evaluation

3.1.1 As-built and after extrusion microstructure

The typical microstructure of the as-built and the extruded bars with different build orientations is presented in Figs. 3 and 4. The microstructure of extruded and heat-treated X direction can be seen in (Fig. 3a) and Z direction in (Fig. 3c). The microstructure of the AM billets is also presented for comparison (Fig. 3b and d, respectively).

The microstructure of the as-built billets is well defined; it shows the characteristic "fish-scale" structure (Fig. 3a) and a track segments morphology (Fig. 3c) due to rapid melting and solidification. The hatching strategy of the laser beam path used in the AM process [2, 3, 9] also contributes to this unique microstructure. The boundaries of

the track segments and fish-scale emphasized due to selective etching of the coarsened Si-rich particles as compare to the other regions. Sizova [12] argued that this feature may be attributed to a transient, slower-growth period during the removal of latent heat from the melt pool or partial re-melting and coarsening of the bottom layer from the top melt pool during consecutive building processes. According to [16] our more common phrase is track segments and fish-scale morphologies.

Although the AM billets underwent ~60% deformation during the extrusion process at 300 °C, the track segments and fish-scale morphologies are still visible, as shown in the Post extrusion (Fig. 3b and d). The unaffected morphology may be attributed to the thermo-mechanical stability of the Si-rich particle at the extrusion temperature. Most of the particles found at the melt pools boundaries are discrete, as shown in Fig. 3b and d. [16, 17] has shown that annealing at 450 °C leads to the formation of continuous thin Si lines about 1 µm in thickness. In contrast to the

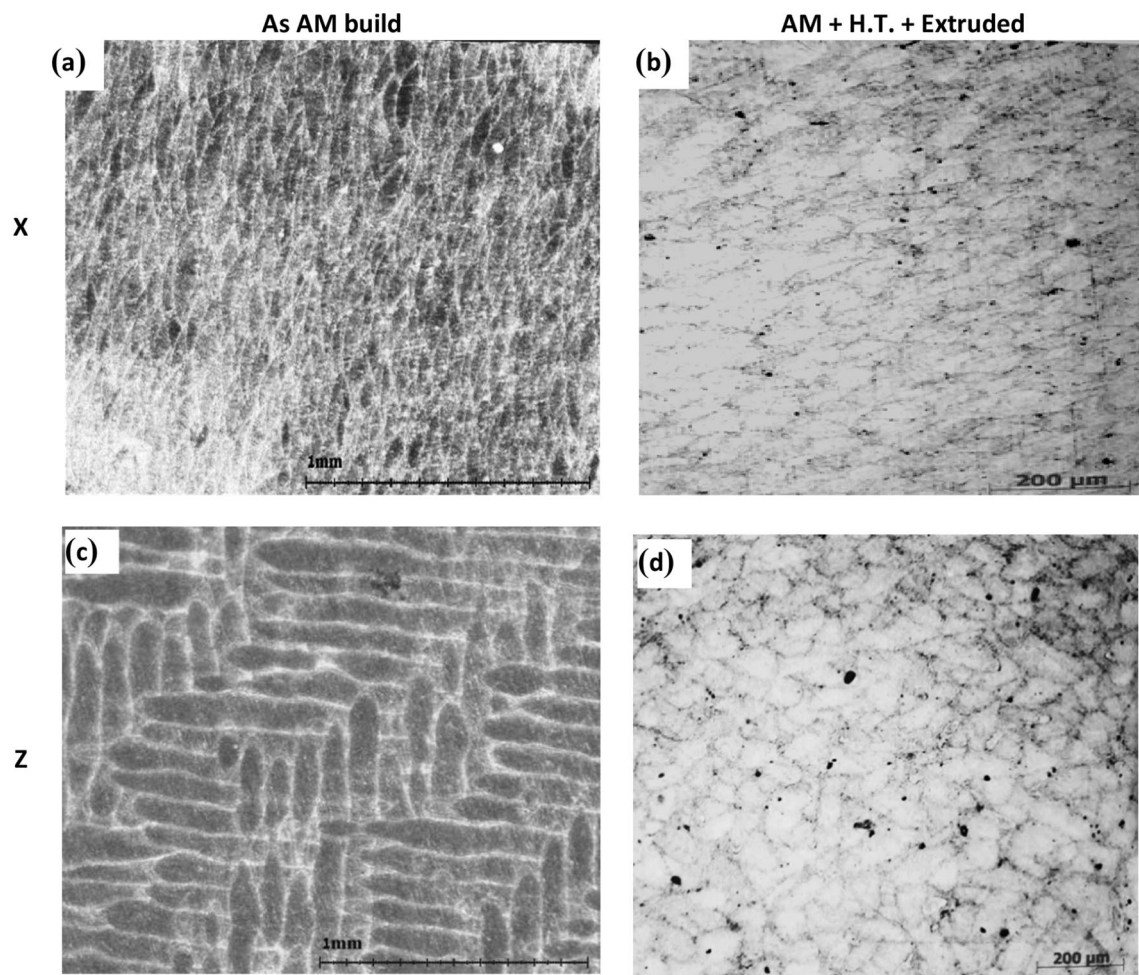


Fig. 3 Microstructure of AM billets with respect to the build directions (a) as build in X direction (b) stress-relieved and extruded X direction (c) as build Z directions (d) stress-relieved and extruded Z directions

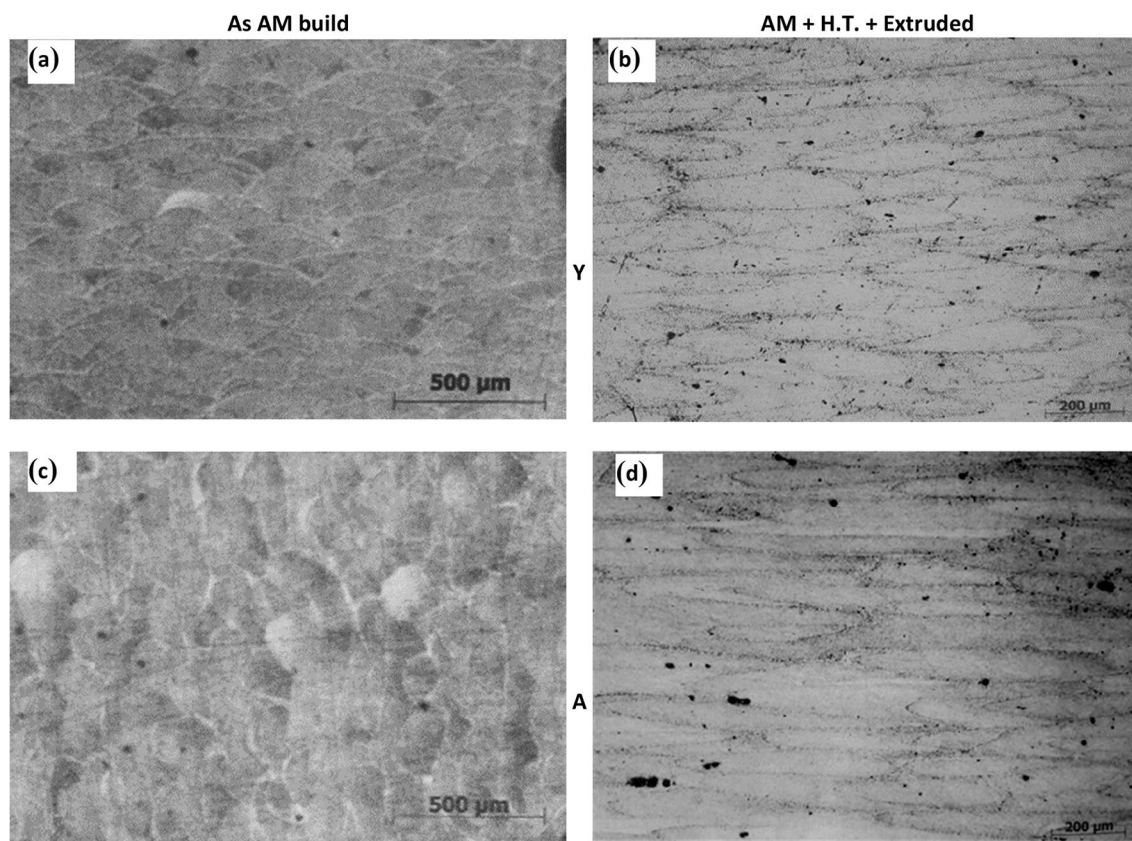


Fig. 4 Microstructure of AM billets with respect to the build directions (a) as build in Y direction (b) stress-relieved and extruded Y direction (c) as build A directions (d) stress-relieved and extruded A directions

stability of the melt pools boundaries, the shape and the size of the melt pools were influenced significantly due to the thermo-mechanical process. A cellular structure is seen in the X (Fig. 3a) and Z (Fig. 3c) and elongated ones in the Y (Fig. 4b) and A (Fig. 4d).

3.2 Microstructure of the as-built AM samples followed by aging

In contrast to the "coarse" microstructure observed after AM, the aging treatment (AG) after solution heat treatment causes a very fine microstructure with an average grain size of about 15 μm . The grain morphology is axis-symmetry for the A and Z directions (Fig. 5a and d, respectively). In contrast, for the X and Y directions (Fig. 5b and c, respectively) elongated grains were observed. As shown, dark particles are also detected; most of them are located at the grain boundaries, which can explain that no grain growth occurred during the SHT at 510 $^{\circ}\text{C}$. These particles are Si-rich phase as detected by X-ray diffraction and reflected at the fracture surface and analyzed by EDAX (as will elaborate later on).

3.3 Mechanical properties evaluation

3.3.1 As AM vs. extruded

For the as-is (As-AM) and the extruded (EX), the stress-strain curves are depicted in Fig. 6a and b, respectively. For the as-AM, the plastic regime is characterized by higher strain hardening compare to the EX. This change is reflected by lower yield stress (YS) compared to the ultimate tensile stress (UTS) for the As-AM, as listed in Table 4. The yield stress is close to ultimate tensile stress (TS) for the EX, which is pointed out on lower strain hardening (Fig. b). However, the influence of the extrusion process is emphasized on the plastic strain, as listed in Table 4. The average elongation for As-AM is $\sim 12\%$, with the lower one for the Z and the higher one for the X. In the EX, significant improvement is achieved for all orientations—the average elongation is 20.3%. Higher YS was obtained for the EX-samples: 285 MPa vs. 249 MPa for the As-AM samples. The average TS of both conditions is similar, ~ 380 MPa, although the EX-samples present a slightly higher distribution of values for the different build directions.

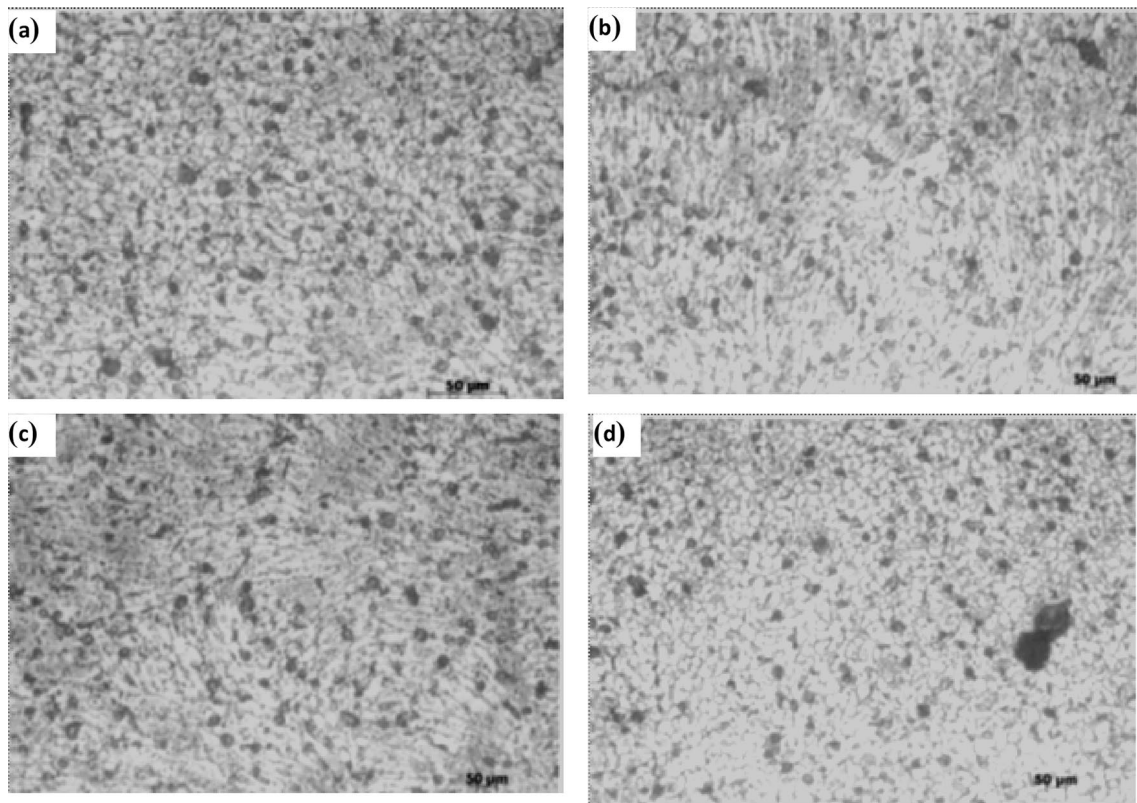


Fig. 5 Microstructure after AM and AG for the different orientations; (a) A, (b) X, (c) Y, (d) Z

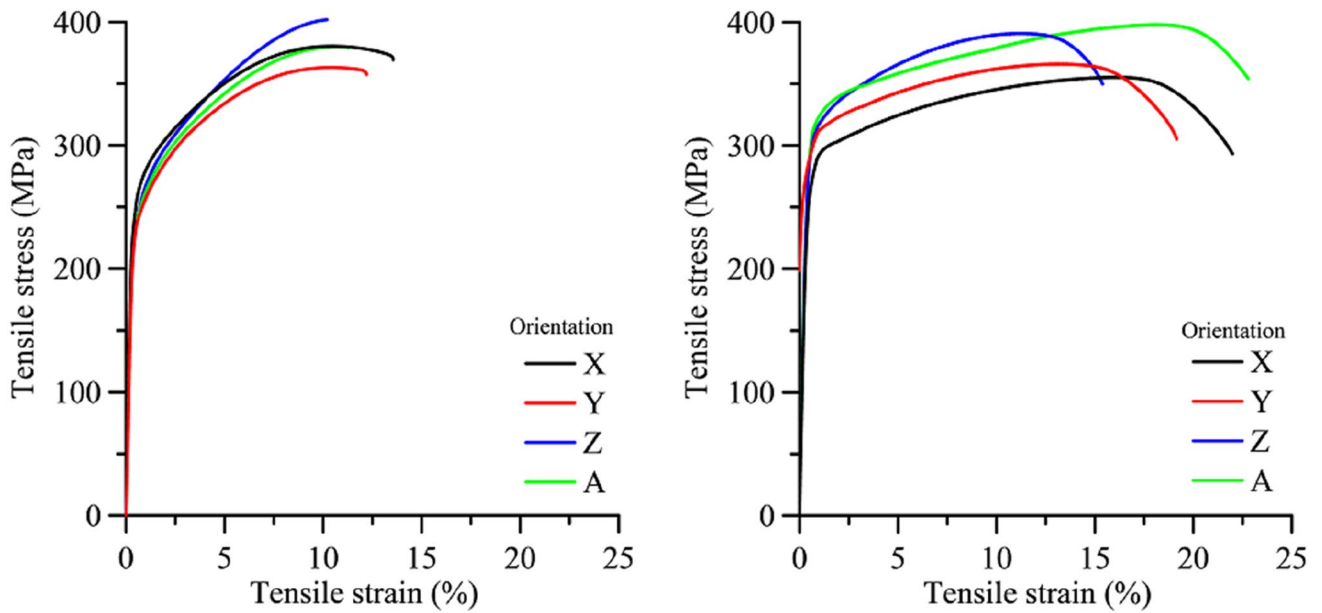


Fig. 6 Stress–strain curves at different orientations for the various metallurgical conditions; (a) as AM, (b) AM following extrusion at 300 °C. X, Y- base plane Z- building direction A 45° to building direction

3.3.2 The influence of the aging process

The properties of the extruded and aged samples (AG) compared to *Y* As-AM are depicted in Fig. 7a and b, respectively. As shown, the AG data for all different orientations are almost identical- no AG effect is noticed. The aging yields a decrease in the YS and the UTS. At the same time, the elongation remains quite similar (Fig. 7b) as compare, for example, to *Y* As-AM orientation with the same tendency as the other orientations. The AG samples exhibited a decrease in the strain hardening potential resulted in YS similar to UTS values. The tendencies and the comparison with the As-AM samples are summarized in Table 5. The poorer effect of the aging treatment is

reflected by the microstructure and the fracture mode, as will be shown later on.

The poor effect of age hardening on the mechanical properties of the EX and AG compare to the As-AM is demonstrated in Table 6. Both YS and UTS are severely decreased by the age-hardening effect even though elongation is a significant increase. Obviously, this increase in elongation is due to the extrusion process and can't be related to the aging process based on the previous tendency shown above. As presented in Fig. 10, the fracture is characterized by fine and deep dimples with the dispersion of Si-rich particles on the fracture surface.

Table 4 Comparison of the tensile mechanical properties of as-built samples and after extrusion

Property/direction	σ_{YS} , MPa		σ_{UTS} , MPa		ϵ_f , %		HV
	As-AM	AM+EX	As-AM	AM+EX	As-AM	AM+EX	AM+EX
Condition	As-AM	AM+EX	As-AM	AM+EX	As-AM	AM+EX	AM+EX
X	260	279	380	356	13.5	22.3	85.5
Y	240	282	360	366	12.1	19.4	85.6
Z	250	290	403	391	10.2	15.7	86.6
A	245	289	381	398	11.5	23.9	83.3
Average	248.8	285	381	377.8	11.8	20.3	

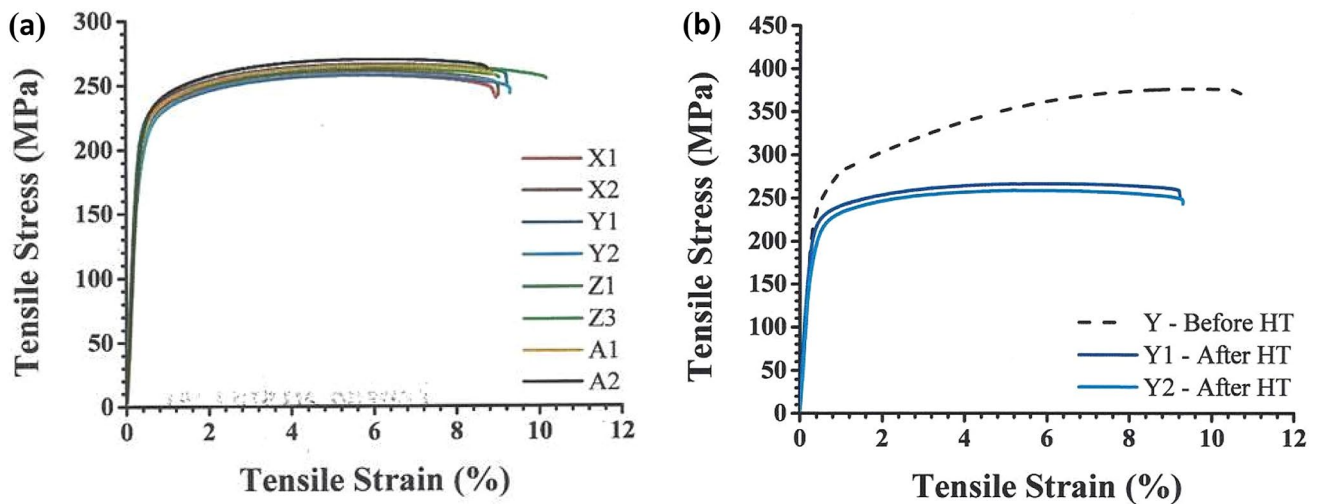


Fig. 7 Stress–Strain curves at different orientations, (a) as AM and aged (AG), (b) comparison of as-built AM and AG, for *Y* orientation. Note the difference of scales

Table 5 Comparison of the tensile mechanical properties of As AM samples and AG

Property/direction	σ_{ys} , MPa		σ_{UTS} , MPa		ϵ_f , %	
	As-AM	AM+AG	As-AM	AM+AG	AS-AM	AM+AG
Condition	As-AM	AM+AG	As-AM	AM+AG	AS-AM	AM+AG
X	260	216	380	260	13.5	9
Y	240	215	360	262	12.1	9.2
Z	250	220	403	263	10.2	9.5
A	245	222	381	267	11.5	9.3

Table 6 Comparison of the tensile mechanical properties of As AM samples and after EX + AG

Property/direction	σ_{ys} , MPa		σ_{UTS} , MPa		ϵ_p %	
	As-AM	AM+EX+AG	As-AM	AM+EX+AG	As-AM	AM+EX+AG
X	260	95	380	178	13.5	31
Y	240	92	360	175	12.1	32
Z	250	88	403	170	10.2	28
A	245	95	381	180	11.5	30

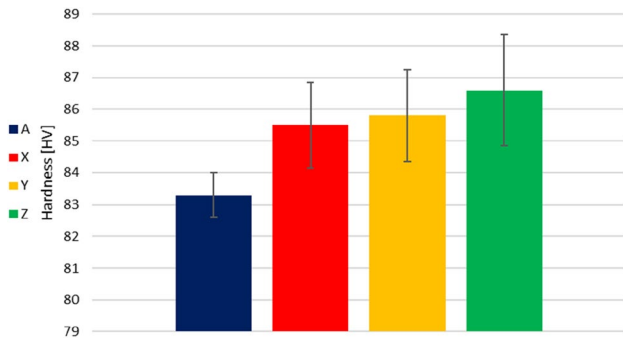


Fig. 8 Vickers hardness of extruded AM billets X, Y- base plane Z- building direction A- 45° to building direction

3.3.3 Hardness evaluation

The hardness results for extrusions of different building directions, as seen in Fig. 8, represent relatively the mechanical properties of the different building directions. The X and Y directions are practically similar due to the build strategy. In contrast, the A direction’s hardness is lower in compliance with the high elongation that characterizes this direction.

3.4 Fracture modes

Figure 9 illustrates the fracture modes for X and A orientations for the as-built and after extrusion conditions. As

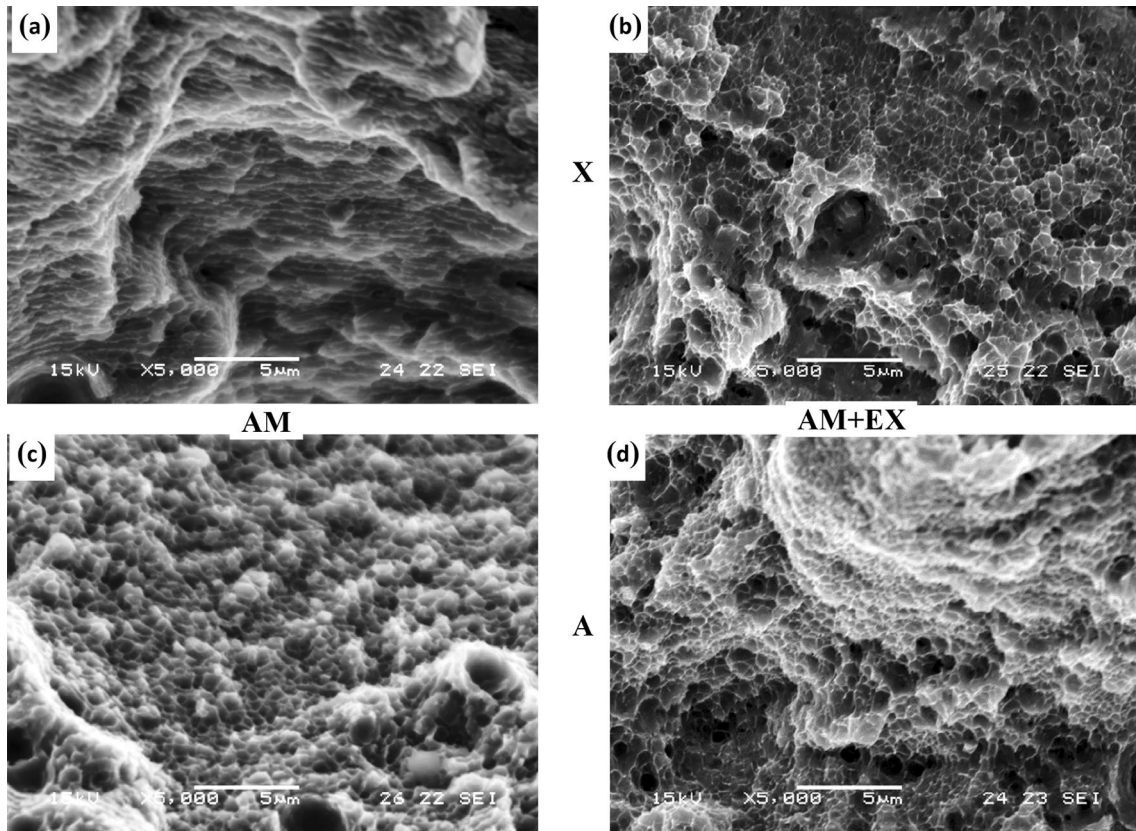


Fig. 9 Fracture modes comparison between AM and after extrusion for different orientations; (a, b) X, (c, d) A

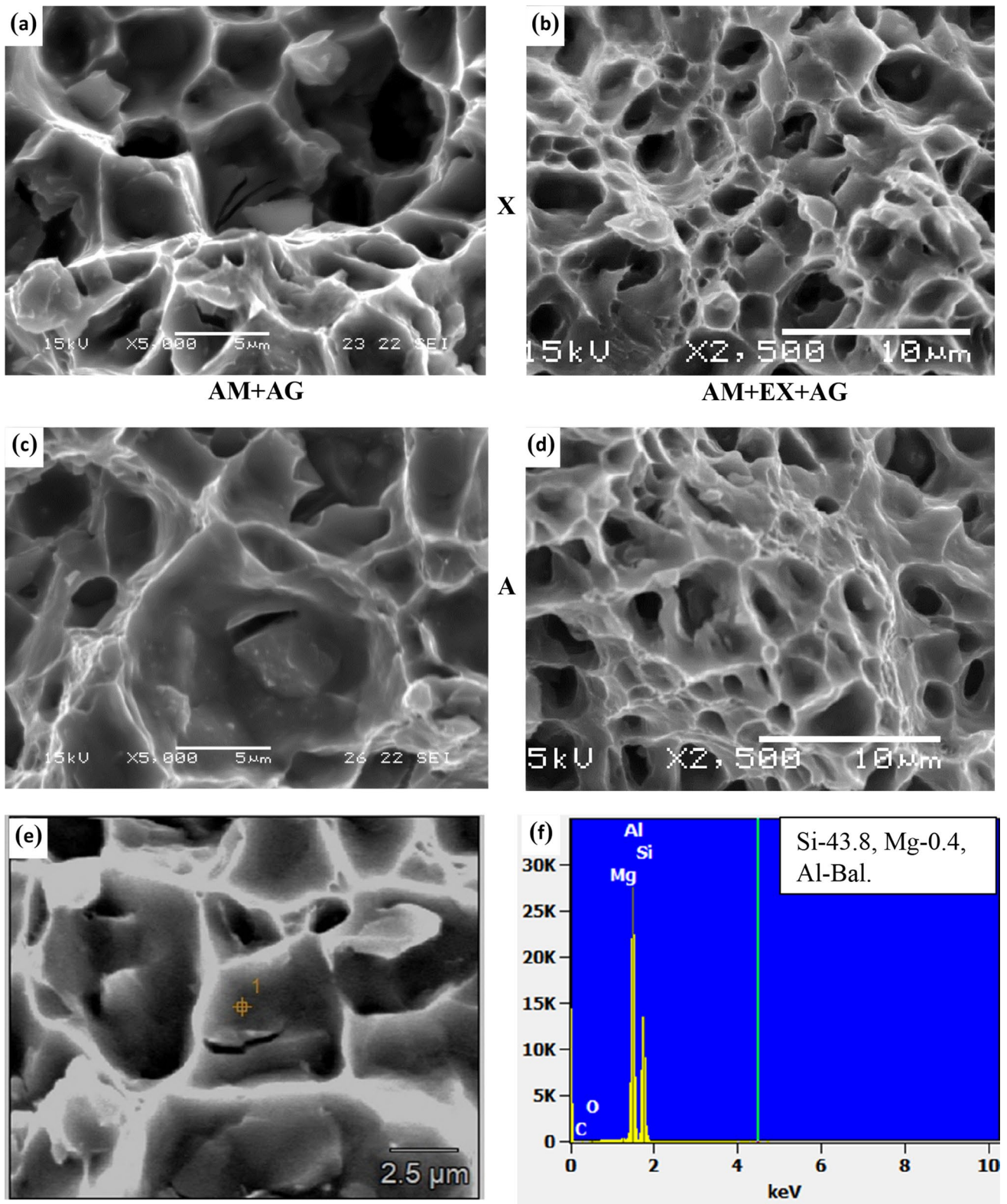


Fig. 10 Fracture modes comparison between AM and after extrusion with AG for different orientations; (a, b) X, (c, d) A, (e) EDAX chemical analysis of cracked particle, (f) spectrum analysis with results

shown for the as-built in the *X* orientation (Fig. 9a), elongated shallow dimples are developed influenced by the AM process, while fine and deep dimples were observed after extrusion (Fig. 9b). The high elongation is manifesting this ductile fracture mode as compared to the as-built condition. For the *Z* orientation, the difference between the as-built (Fig. 9c) and after extrusion (Fig. 9d) is related to the more fracture energy obtained for the latter as reflected by fine and deep dimples (Fig. 10).

3.5 Discussion

This paper reports for the first time about the extrusion of additively manufactured AlSi10Mg alloy. SLM AM billet was hot extruded and aged, to elucidate the microstructure and mechanical behavior of extruded AM material. In previous similar research it was reported that microstructure was refined during hot working due to recrystallization. Much lower flow stress values were found compared to conventional cast + HIPed material, while flow stress was reduced by more than 40%. In this research it was found that the strength of AM extruded samples was higher by 30–40% of the as AM samples or casts of the same alloy (See Table 7). The elongation to fracture of the extruded AM samples was found to be four times higher than of the cast alloy. The assumption that the mechanical properties of extruded fine grains AM would be enhanced due to Hall–Petch law was proven. Preferred uni-directional microstructure that can be observed in the as extruded (Fig. 4b, d) can also explain the difference in mechanical properties according to AM build direction. It is quite obvious that the preferred orientation of AM direction *Y* (Fig. 4b) is much noticeable than of *A* direction (Fig. 4d). Indeed, both strength and elongation were improved by elevated temperature extrusion, as shown in Table 7, compared to as-cast and as-built AM. The YS of additively manufactured and extruded (AM + EX) was about 50% higher in all building directions. The influence of building direction on the UTS of the extruded AM billets was found to be dramatic. It was found that the *A* building direction (45° to *Z* direction) is characterized by the optimal combination of strength and ductility. Engineers might use this phenomenon in cases where extruded profiles should have an extreme combination of mechanical properties. Further research is suggested to gain an understanding for this phenomenon. Unfortunately, the aging process had impaired the mechanical properties. In all cases, both strength and ductility were decreased by aging treatment. The reason for that wasn't found by metallography and fractography that were used in this research. To exploit the opportunities of extruding AM billets, one must consider the cost of producing an AM billet vs. using a cast one. Although additive manufacturing of an extrusion billet takes more time, it might be worth it if the cost of crucible, casting molds and the need

Table 7 Comparison of mechanical properties: this research and literature [6, 9]

Source	Direction/property	σ_{ys} , MPa	σ_{UTS} , MPa	ϵ_f , %	HV
Current research AM + EX	<i>X</i>	279	356	22.3	85.5
	<i>Y</i>	282	366	19.4	85.6
	<i>Z</i>	290	391	15.7	86.6
	<i>A</i>	289	398	23.9	83.3
Ref [10]	As cast	165	315	4	80
Ref [6]	AM <i>XY</i> direction	185	267	22.8	94
Ref [6]	AM <i>Z</i> direction	184	273	18.3	94
Ref [15]	6061-T6	255	290	12	107

to recycle metal are compared to 3D printing of multiple billets in one cycle with no need of molds and very low loss of material. The mechanical properties of hot extruded AM AlSi10Mg was found to be superior in comparison to 6061-T6 (see Table 7) therefore, it generates an opportunity to manufacture AlSi10Mg parts for tough mechanical use.

4 Conclusions

Plastic deformation of AM billets is not a standard procedure since manufacturers see AM as a manufacturing process of prototypes or final product. The authors took advantage of the fine microstructure and texture of the SLM AM billet to improve the mechanical properties of AlSi10Mg products by hot extrusion.

- Extruded AM samples have improved mechanical properties in comparison to as AM or casts of this alloy.
- Additively manufactured samples in 45° to the building direction *A* show's enhanced mechanical properties. It is recommended to design a building route and directions to exploit the *A* direction (45°) to the most important direction in additively manufactured and extruded future processes.
- Manufacturing extrusion billets by additive manufacturing can be considered a means to gain better mechanical properties of the final products.
- The aging process is not recommended for extruded AM applications until a further understanding of this issue. The stress relief was found to be useful to increase formability by extrusion.
- Further research is needed to exploit the influence of the billet building route and direction on the final mechanical properties.

Acknowledgements The authors wish to thank “Sharon Tuvia (1982) Ltd” for supplying the AlSi10Mg AM samples and “Alubin Extrusions Ltd” for the design and manufacturing of the extrusion micro-press. We also thank R. Shneck, for the valuable support, and I. Benishti, and S. Levi for excellent metallography work. The authors are grateful to E. Millionshckik for their valuable technical contributions. The authors also appreciate the support of E. Tiferet and Y. Ganor for AM samples preparation and to S. Samuha for the scientific support.

References

1. Wang Z, Ummethala R, Singh N, Tang S, Suryanarayana C, Eckert J, Gokuldoss PK (2020) Selective laser melting of aluminum and its alloys. *Materials* 13:4564. <https://doi.org/10.3390/ma13204564>
2. Voncina M, Mrvar P, Medved J (2006) Thermodynamic analysis of AlSi10Mg alloy. *RMZ Mater Geo Environ* 52(3):621–633
3. Schade C, Dunkley JJ (2015) Atomization, powder metallurgy. *ASM Int ASM Handb* 7:58–71
4. Nahmany M, Hadad Y, Aghion E, Stern A, Frage N (2019) Microstructural assessment and mechanical properties of electron beam welding of AlSi10Mg specimens fabricated by selective laser melting. *J Mater Process Technol* 270:228–240
5. Yang Y, Lu C, Peng S, Shen L, Wang D, Qi F, Shuai C (2020) Laser additive manufacturing of Mg-based composite with improved degradation behavior. *Virtual Phys Prototyp* 15(3):278–293. <https://doi.org/10.1080/17452759.174838>
6. Nahmany M, Rosenthal I, Benishti I, Frage N, Stern A (2015) Electron beam welding of AlSi10Mg workpieces produced by selected laser melting additive manufacturing technology. *Addit Manuf* 8:63–70
7. Kazanowski P (2012) Evaluation of process mechanism and parameters. In: 10th International Aluminum Extrusion Technology Seminar, Miami
8. Heeling T, Wegener K (2018) The effect of multi-beam strategies on selective laser melting of stainless steel 316L. *Addit Manuf* 22:334–342
9. Bremen S, Meiners W, Diatlov A (2012) Selective laser melting, a manufacturing technology for the future. *Laser Tech J* 9(2):33–38. <https://doi.org/10.1002/latj.201290018>
10. Mertens A, Dedry O, Deuter D, Rigo O, Comebackers J (2015) Thermal treatment of AlSi10Mg processed by laser beam melting. In: Bourell D (ed) *Proceedings of the 6th International Solid Freeform Fabrication Symposium*. University of Texas at Austin, Austin, TX, p 1007
11. Nahmany M (2018) Electron beam welding of additive manufactured AlSi10Mg alloy: optimal welding parameters, microstructure of the weld metal and mechanical properties of joints. PhD Thesis, Ben-Gurion University of the Negev
12. Sizova I, Sviridov A, Bambach M, Eisentraut M, Hemes S, Hecht U, Marquardt A, Leyens C (2021) A study on hot-working as alternative post-processing method for titanium aluminides built by laser powder bed fusion and electron beam melting. *J Mater Process Tech* 291:117024
13. Martina F, Colegrover PA, Williams SW, Meyer J (2015) Microstructure of interposes rolled wire + Arc additive manufacturing Ti-6Al-4V components. *Met Mat Tran A* 46A:6103
14. Michla D, Sydow B, Bambach M (2020) Ring rolling of pre-forms made by wire-arc additive manufacturing. *Procedia Manuf* 47:342–348
15. Anderson K, Weritz J, Kaufman JG (2019) Properties and selection of aluminum alloys. ASM International, V2B, ISBN: 978-1-62708-210-5
16. Sizova I, Bambach M (2018) Hot workability and microstructure evolution of pre-forms for forgings produced by additive manufacturing. *J Mater Process Tech* 256:154–159
17. Manfredi D, Calignano F, Krishnan M, Canali R, Ambrosio E, P, Biamino S, Ugues D, Pavese M, Fino P (2014) Additive Manufacturing of Al Alloys and Aluminum Matrix Composites (AMCs), Additive Manufacturing of Al Alloys and Aluminium Matrix Composites (AMCs), Chapter 1, <https://doi.org/10.5772/58534>

Publisher's Note Springer Nature remains neutral with regard to jurisdictional claims in published maps and institutional affiliations.